A pyramid sensor based AO system for Extremely Large Telescopes

F. Quirós-Pacheco[1,a], E. Pinna[1], S. Esposito[1], C. Arcidiacono[2], G. Agapito[1], S. Rabien[3]

[1]INAF – Osservatorio Astrofisico di Arcetri, Largo E. Fermi 5, 50124 Firenze, Italy

[2]INAF – Osservatorio Astronomico di Bologna, Via Ranzani 1, 40127 Bologna, Italy

[3]Max Planck Institute für extraterrestrische Physik, Gießenbachstr., 85748 Garching, Germany

Abstract. Since the introduction of the pyramid wavefront sensor in the mid 90s, various authors have shown both theoretically and with the aid of simulations that pyramid sensors can achieve a better performance than traditional Shack-Hartmann wavefront sensors. Recently the First-Light Adaptive Optics system (FLAO) at the Large Binocular Telescope demonstrated excellent on sky performance achieved with a pyramid based system. Motivated by these results, we will present in this paper a first heuristic analysis scaling up the FLAO performance to the case of an Extremely Large Telescope (ELT). We support our arguments with preliminary numerical simulations for the case of the European ELT using the M4 adaptive corrector design and a properly matched pyramid sensor. Such a system could be used as a first-light natural guide-star AO system for the European ELT offering the advantages of a demonstrated AO system with practically off-the-shelf technology.

1. Introduction

The pyramid sensor was introduced by Ragazzoni in 1996 [1]. Since then, various authors studied the pyramid Wave-Front Sensor (WFS) behavior in theory and with numerical simulations, in particular showing that the pyramid WFS could achieve a better performance than the Shack-Hartmann WFS for a given reference star flux [2-5]. These predictions were later confirmed in the laboratory with the High Order Testbench (HOT) experiment [6], and later on by the First Light Adaptive Optics (FLAO) system of the Large Binocular Telescope (LBT), featuring a Deformable Secondary Mirror (DSM) with 672 actuators and a pyramid WFS with a maximum sampling of 30×30 subapertures [7].

The on-sky FLAO results —such as H band SR higher than 80%, image contrast better than 10^{-4}, and loop closure down to 17.5 R-magnitude star— set a new standard for ground-based astronomical AO systems [8]. These results showed that pyramid sensors —and also large

[a] e-mail : fquiros@arcetri.astro.it

adaptive mirrors— are mature technologies to be used in the design of future AO systems for Extremely Large Telescopes (ELTs). This is the path followed by the Great Magellan Telescope (GMT), a 25-m ELT project comprising a "segmented" DSM with 4704 actuators, and a ~90×90 pyramid sensor for the Natural Guide Star (NGS) AO mode [9].

Motivated by the FLAO results, we will present in Section 2 a first heuristic analysis scaling up the FLAO performance to the case of the European ELT [10]. We will then present in Section 3 the results of preliminary numerical simulations estimating the performance that could be obtained on the ELT using the M4 adaptive corrector [11] and a properly matched pyramid WFS. As we will discuss, such a system could be used as a first-light natural guide-star AO system for the European ELT offering the advantages of a demonstrated AO system with practically the technology available now.

2. Scaling the performance of the FLAO system to an ELT

The results achieved by the FLAO system at the LBT can be scaled to the case of an ELT using simple arguments. Let us consider an ELT of 42m in diameter, which is exactly 5 times larger than the 8.4m diameter of one arm of the LBT. We can see this ELT as made up of approximately 5×5 LBT patches, as illustrated in Figure 1.

The "low-order" modes on the ELT will have larger spatial scales than on the LBT, and so they will disturb the images with some additional turbulence power. However, the time scales for these modes on the ELT will be, according to the Taylor hypothesis, lower than on the LBT. Therefore, it is reasonable to assume that the correction of such new low-order modes will not be a concern given an appropriate sampling and frame rate.

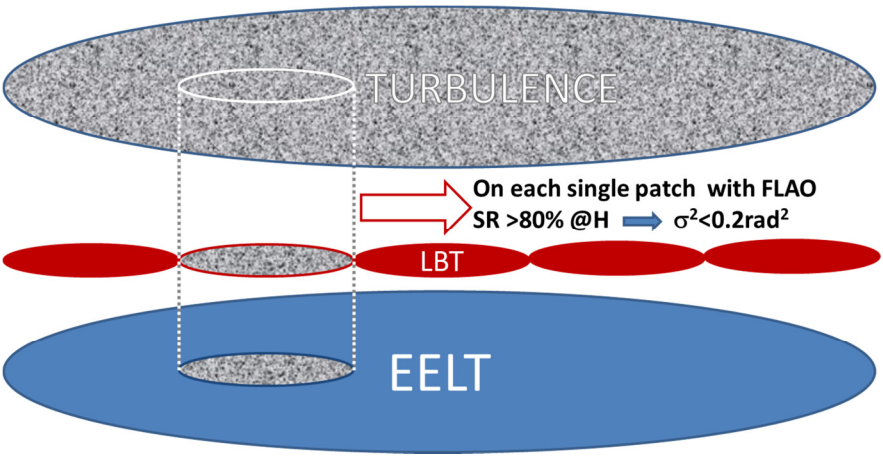

Figure 1. A sketch of the 42-m diameter ELT seen as made up of 5×5 8.4m diameter patches.

Table 1. Scaling LBT's FLAO high-order system parameters to produce the same Strehl Ratio on the ELT.

Telescope	D (m)	#modes	Subaps.	Framerate	Modulation
LBT	8.4	400	30×30	1kHz	$\pm 3\lambda/D$
ELT	42	10000	150×150	1kHz	$\pm 15\lambda/D$

Let us consider a deformable mirror on the ELT having the actuator spacing of the LBT's DSM, which is ~0.3m once projected on the LBT's primary mirror. Keeping the actuator spacing constant ensures the correction up to the same spatial scales in both cases. In terms of modes, this consideration leads to an increment of 5^2 in the number of controlled modes: the 400 modes typically used for high-order correction on the LBT will be equivalent to a total of 10000 modes on the ELT. The WFS sampling must be scaled accordingly from 30×30 to 150×150 subapertures. Also, in order to have the same pyramid WFS sensitivity, the on-sky angle of modulation must be kept constant. Expressing the pyramid modulation radius in multiples of λ/D (where λ is the WFS working wavelength and D the telescope diameter), a modulation radius of $15\lambda/D_{ELT}$ on the ELT will be equivalent to the typically used modulation radius of $3\lambda/D_{LBT}$ on the LBT. Using these numbers of actuators, subapertures, and pyramid modulation on the ELT will produce the same level of performance achieved at the LBT in terms of Strehl Ratio (see Table 1).

It is interesting to note that the performance in terms of Point Spread Function (PSF) contrast will be improved on the ELT. Let us approximate the contrast $C(\theta)$ at a distance θ from the central peak by:

$$C(\theta) = \frac{I(\theta)}{I(0)} = \frac{I_{DL}(\theta)+\Delta I(\theta)}{I(0)} \approx \frac{\Delta I(\theta)}{I(0)} \quad (1)$$

where $I_{DL}(\theta)$ stands for the intensity pattern that would be obtained in diffraction-limited conditions, and $\Delta I(\theta)$ stands for the additional intensity due to the AO residuals. The last approximation in Eq. (1) is reasonable where the AO residuals dominate.

Assuming that we are observing a given star with the LBT telescope achieving a contrast of $C_{LBT}(\theta)$. When observing the same star with the ELT, the total received flux will increase by a factor $k^2 = (D_{ELT}/D_{LBT})^2 = 25$. The energy scattered in the dark halo by high spatial frequency residuals of the AO system will simply scale as the flux, so $\Delta I_{ELT}(\theta) = k^2\, \Delta I_{LBT}(\theta)$. This is true of course under the assumption that the high-order correction achieved on the ELT is exactly the same as on the LBT given the proposed scaled AO system parameters. On the other hand, the peak of the PSF on the ELT, $I_{ELT}(0)$, will increase for two different reasons: (a) the already mentioned increment of received flux, so a factor k^2; (b) the higher energy concentration due to the smaller diffraction-limited core of the ELT's PSF, causing an additional factor of k^2. In the end, the final contrast on the ELT will be improved by:

$$C_{ELT}(\theta) \approx \frac{\Delta I_{ELT}(\theta)}{I_{ELT}(0)} = \frac{k^2 \Delta I_{LBT}(\theta)}{k^4 I_{LBT}(0)} \approx \frac{C_{LBT}(\theta)}{\left(\frac{D_{ELT}}{D_{LBT}}\right)^2} = \frac{C_{LBT}(\theta)}{25}. \quad (2)$$

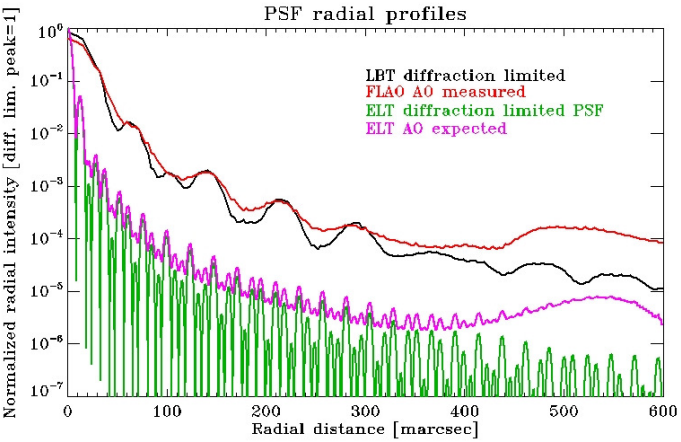

Figure 2. (Color on-line) Profiles of the LBT's diffraction-limited PSF (black line), measured FLAO's high-order corrected PSF (red line), 42m ELT's diffraction-limited PSF (green line), and the estimated ELT's AO-corrected PSF (pink line).

We verified this gain in PSF contrast with a simple analysis using as initial data a high-order corrected PSF with SR of >80% in H band acquired during the on-sky commissioning of the LBT's FLAO system [8]. We obtained a rough estimation of the AO residuals as $\Delta I_{LBT}(\theta) = I_{LBT}(\theta) - I_{DL,LBT}(\theta)$, where $I_{LBT}(\theta)$ is the average intensity measured on the AO-corrected image at a distance θ, and $I_{DL,LBT}(\theta)$ is the average intensity of the diffraction-limited PSF at the same angle. We computed this quantity in the minima of the diffraction-limited profile and then we interpolated the data for the other values of θ. We finally estimated the expected profile of the AO-corrected PSF on the ELT as $I_{ELT}(\theta) = I_{DL,ELT}(\theta) + \Delta I_{ELT}(\theta)$. Figure 2 shows the profiles of $I_{LBT}(\theta)$, $I_{DL,LBT}(\theta)$, $I_{DL,ELT}(\theta)$, and the estimated $I_{ELT}(\theta)$. Note that the contrast at θ~0.4 arcsec on the ELT's AO-corrected PSF is ~4×10^{-6}; that is, a factor k^2=25 better than the LBT's AO-corrected PSF of ~10^{-4}, as expected.

3. A first-light AO system for the E-ELT: preliminary simulations

In the previous section we showed that in order to have the same FLAO performance on a 42m ELT it would take an AO system with ~10^4 actuators and 150×150 subapertures. The current ~40m design of the European ELT (E-ELT) comprises a ~2.5m deformable mirror (DM) of ~6000 actuators with a pitch of 31.5mm [11]. Projected onto the primary mirror, the ~0.5m actuators pitch can be properly matched with a WFS having ~80×80 subapertures. We will present in this section some preliminary numerical simulations of an 80×80 pyramid-based AO system that could be used as a first-light AO system for the E-ELT.

Table 2. Summary of simulation parameters used to estimate the performance of a pyramid-based first-light AO system for the E-ELT.

Telescope	42m in diameter, with a central obscuration of 30% in diameter
Turbulence	Von-Karman turbulence with a seeing of 0.8", L_0=50 m, and a wind speed of 12.5m/s evolving according to the Taylor hypothesis.
Pyramid sensor	80×80 subapertures; wavefront sensing at 600 or 750 nm; noiseless CCD detector; sampling frequency of 1kHz.
Deformable mirror	Correction based on KL modes; no realistic influence functions modelled.
Temporal controller	Simple integrator (g=0.8). Total delay of 1 frame.

The general parameters taken into account in our simulations are summarized in Table 2. The 80×80 pyramid WFS has been modelled with a full Fourier optics code comprising tilt modulation. Two sensing working wavelengths have been considered: 600 nm and 750nm. We assumed a CCD detector with no Read-Out Noise (RON), which is close to the current status of EMCCD technology [12]. For the purpose of flux calculations, we have considered an overall transmission (telescope + WFS board including CCD quantum efficiency) of $0.9^5 \times 0.5 = 0.3$. Regarding the DM, no realistic actuator influence functions were taken into account. We have assumed that the mirror can produce theoretical Karhunen–Loève (KL) modes. A correction with a maximum of 4016 KL modes has been simulated.

The pyramid modulation allows us to adjust the sensor sensitivity to the atmospheric conditions and, consequently, to tune up the correction performance. As shown in Figure 3, a modulation of ±5λ/D is sufficient for bootstrapping the AO correction on a 42m telescope providing after convergence a residual variance of 4.8 rad^2 @ 600nm. For comparison, the theoretical residual variance after perfect removal of the first 4016 Zernikes is 3 rad^2 @ 600nm.

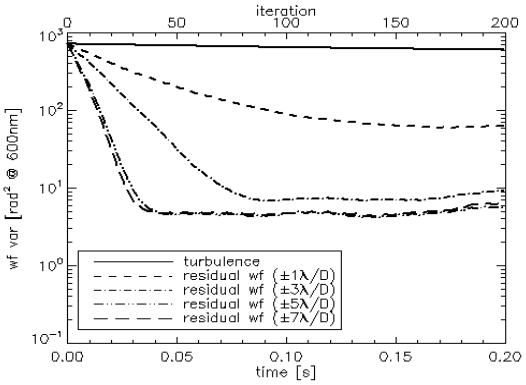

Figure 3. Pyramid WFS bootstrapping with different modulations (high-flux conditions).

Figure 4(Left) shows the performance of the simulated AO system in terms of Strehl Ratio (SR) in H band as a function of the star magnitude, and for the two considered sensing wavelengths. The applied modulation was ±5λ/D in all cases. Also, because no RON was introduced in the simulations, fine-tuning of the sampling frequency was not necessary. On the other hand, it was required to reduce the number of controlled modes for fainter guide stars. Figure 4(Right) shows the modal residual variances (rad^2 @ 750nm) attained a different flux levels.

As expected, wavefront sensing at 750nm results in a better performance because the PSF atop the pyramid vertex at 750nm still benefits from some partial AO correction (~14% of SR for the 10^{th}-star magnitude case) whereas at 600nm it is basically seeing-limited. Hence, the pyramid sensor suffers a reduction in sensitivity −which is inversely proportional to the FWHM of the PSF− in the latter case.

Figure 5 shows the best AO-corrected PSF obtained under high-flux conditions (10^{th} mag). The profiles of the AO-corrected and the diffraction-limited PSFs are also shown. The AO-corrected PSF with a SR in H band of 67% exhibits a diffraction-limited core of 8mas FWHM, and a residual halo at ~300mas due to the uncorrected turbulence. Note the deep annular region where the non-aliased correction offered by the pyramid sensor achieves a maximum contrast of ~5×10^{-5} at a radial distance of ~250mas from the central peak.

The sky coverage offered by an NGS AO system is linked to the efficiency of the wavefront sensing and correction in photon-starving regimes. An AO system based on the pyramid sensor is an efficient solution since the pyramid sensor offers a larger sensitivity in the faint end with respect to other available sensors, pushing further the limiting magnitude [2,3]. An enhancement in the limiting magnitude translates into an improvement of the sky fraction accessible with adaptive optics. Single-conjugate AO corrects efficiently on a small patch, the angular size depending on the strength of the atmospheric turbulence and vertical distribution, and on the number of corrected modes: the isoplanatic angle.

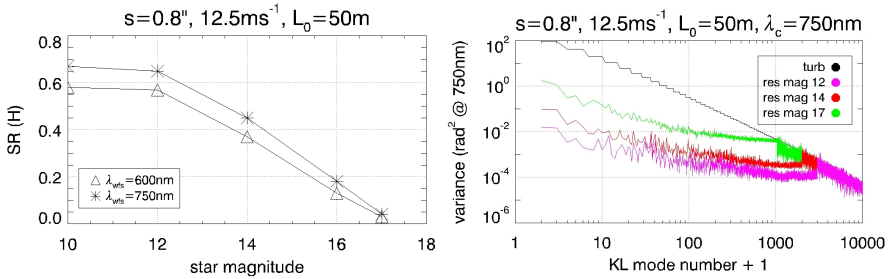

Figure 4. (*Left*) Strehl Ratio in H band versus star magnitude (V vs. R band sensing). (*Right*) (Color on-line) Residual modal variances @ 750nm attained at different flux levels. The number of KL modes controlled were 4016 (mag10), 3000 (mag12), 2014 (mag14-16), and 1030 (mag17). A sampling frequency of 1kHz, a tilt modulation of ±5λ/D, and a gain of 0.8 were used at all flux levels.

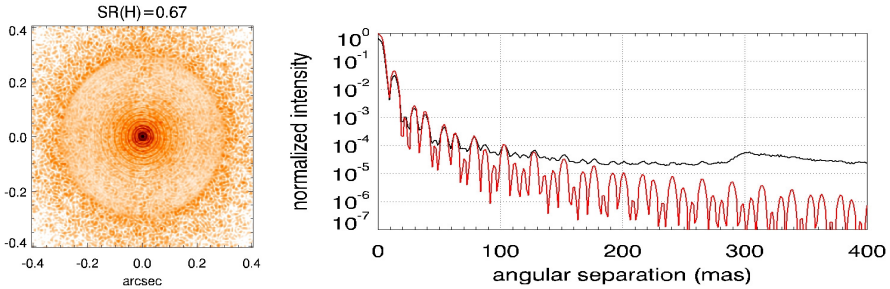

Figure 5. (*Left*) AO-corrected PSF in H band obtained with a 10th R-magnitude guide star. (*Right*) (Color on-line) Comparison between the diffraction-limited PSF (red curve) and the AO-corrected PSF profiles (black curve). Profiles normalized to the diffraction-limited peak.

We computed the sky coverage using as reference a sample of 830 galaxies at z~3 in 16 different fields located at high galactic latitude [13]. We considered two isoplanatic angles of 30 and 40 arcsec in K band, defined as the angular distance at which the SR is e^{-1} times the SR on the NGS. For each galaxy we then associated the SR in K band resulting from the combination of NGS brightness and their angular separation.

Figure 6 shows the on-axis SR in K band as a function of the NGS brightness, and the sky coverage results for different SR values. For example, we may select a threshold of 10% of SR to define whether a particular sky direction has coverage or not. With this condition, we find sky coverage values for the considered sample of 20% to 35% (for 30 and 40 arcsec respectively).

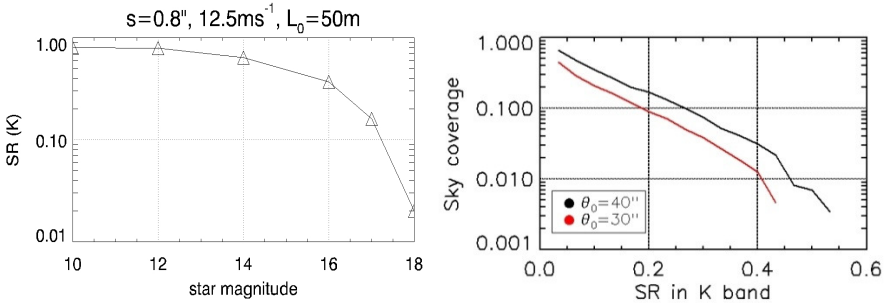

Figure 6. (Left) Strehl Ratio in K band versus star R-magnitude. (Right) Sky coverage for two assumed isoplanatic angles in K band (30 and 40 arcsec), for the sample of 830 galaxies considered.

4. Conclusions

The performance attained with the FLAO system of the LBT has demonstrated the advantages of a pyramid-based AO system on an 8m-class telescope. The maturity of this technology has reached such a level to be considered as part of a first-light natural-guide-star AO system for the incoming ELTs. In the case of the European ELT, we have found with some preliminary numerical simulations that an 80×80 pyramid WFS coupled to the M4 adaptive corrector would provide under high-flux conditions a SR of 67% in H band (0.8" seeing) and a maximum (raw) contrast of 5×10^{-5}. Furthermore, this pyramid WFS could be realized with already-existing EMCCD technology due to its more compact imaging requirements with respect to an equivalent Shack-Hartmann sensor.

5. References

1. R. Ragazzoni, "Pupil plane wavefront sensing with an oscillating prism", J. Mod. Opt. **43**, 289-293 (1996)
2. R. Ragazzoni, J. Farinato, "Sensitivity of a pyramidic wave front sensor in closed loop adaptive optics", A&A **350**, L23-L26 (1999)
3. S. Esposito, A. Riccardi, "Pyramid wavefront sensor behaviour in partial correction adaptive optic systems", A&A **369**, L9-L12 (2001)
4. C. Verinaud, "On the nature of the measurements provided by a pyramid wave-front sensor", Opt. Commun. **233**, 27-38 (2004)
5. C. Verinaud, M. Le Louarn, V. Korkiakoski, M. Carbillet, "Adaptive optics for high-contrast imaging: pyramid sensor versus spatially filtered Shack-Hartmann sensor", MNRAS **357**, L26-L30 (2005)
6. E. Pinna, A. T. Puglisi, F. Quirós-Pacheco, L. Busoni, A. Tozzi, S. Esposito, E. Aller-Carpentier, M. Kasper, "The pyramid wavefront sensor for the High Order Testbench (HOT)", in *Adaptive Optics Systems*, eds. N. Hubin, C. E. Max, P. L. Wizinowich, Proc. SPIE **7015**, 701559 (2008)
7. S. Esposito, et. al., "Laboratory characterization and performance of the high-order adaptive optics system for the Large Binocular Telescope", Appl. Opt. **49**, 31, G174-G189 (2010)
8. S. Esposito, et. al., "Large Binocular Telescope Adaptive Optics System: New achievements and perspectives in adaptive optics", in *Astronomical Adaptive Optics Systems and Applications IV*, eds. R. K. Tyson, M. Hart, Proc. SPIE **8149**, 814902 (2011)
9. A. H. Bouchez, "The Giant Magellan Telescope AO program", This conference, (2011)
10. R. Gilmozzi, J. Spyromilio, "The 42m European ELT: status", in *Ground-based and Airborne Telescopes II*, eds. L. M. Stepp, R. Gilmozzi, Proc. SPIE **7012**, 701219 (2008)
11. D. Gallieni, et. al., "Voice-coil technology for the E-ELT M4 Adaptive Unit", 1st AO4ELT conference, 06002 (2010)
12. P. Feautrier, "A decadal survey of AO wavefront sensing detector developments in Europe", This conference, (2011)
13. C. C. Steidel, K. L. Adelberger, A. E. Shapley, M. Pettini, M. Dickinson, M. Giavalisco, "Lyman Break Galaxies at Redshift z~3: Survey Description and Full Data Set", Astrophys. J., **592**, 2, 728-754 (2003)